

Nature of Dynamic Processes Associated with the S_N1 Reaction Mechanism

Kevin S. Peters

Department of Chemistry and Biochemistry, University of Colorado at Boulder, Boulder, Colorado 80309-0215

Received September 19, 2006

Contents

1. Introduction	859
2. Background	860
2.1. Formulation of the Intermediacy of Ion Pairs	860
2.2. Role of Solvent Participation in S _N 1	860
2.3. Nucleophilic Reactivities	861
3. Electronic Structure Theory for Bond Heterolysis	861
3.1. Early Theoretical Considerations	861
3.2. Valence-Bond Approach for Organic Reactivity	862
3.3. Theoretical Studies of the Influence of Solvent on Bond Heterolysis	862
3.4. Empirical Valence-Bond Model with Explicit Solvent Interaction	863
3.5. Quantum Calculations	863
4. Kinetic Theories	864
4.1. Transition-State Theory	864
4.2. Kramers Theory	864
4.3. Grote–Hynes Theory	865
4.4. Large Amplitude Motions—A Test of Hydrodynamic Theories	865
4.5. Grote–Hynes Theory for Unimolecular Ionic Dissociation	866
4.6. Nonequilibrium Solvation in <i>tert</i> -Butyl Chloride Heterolysis	866
5. Theoretical Perspective on Ion Pair Interconversions	867
6. Experimental Studies for the S _N 1 Mechanism	867
6.1. Kinetic Studies for Benzhydryl Derivatives	867
6.2. Role of Polarization Caging in the Collapse of the CIP	868
6.3. Solvent Control of Contact Ion Pair Separation	869
6.4. Parameters Controlling Nucleophilicity	870
7. Application of Marcus Theory to the S _N 1 Mechanism	871
8. Concluding Remarks	871
9. Acknowledgments	872
10. References	872



Kevin Peters was born in Ponca City, Oklahoma, in 1949. After obtaining his B.S. from the University of Oklahoma in 1971, he pursued his graduate studies with Professor Ken Wiberg in the Department of Chemistry, Yale University, obtaining his Ph.D. in 1975. After 3 years of postdoctoral studies with Professor Fred Richards at Yale University and with Professor Merethe Applebury, Princeton University, and Dr. Peter Rentzepis, Bell Laboratory, he joined the faculty of the Department of Chemistry, Harvard University, in 1978. He then moved to the Department of Chemistry and Biochemistry, University of Colorado at Boulder, in 1984. His research interests continue to be in the application of laser methodologies to the study of organic reaction mechanisms.

The subject of this review is not to recount the development of this field of study; the development has already been chronicled by Raber, Harris, and Schleyer, and more recently by Richard.^{9,10} Instead, this review delves into the recent advances in our understanding of the fundamental nature of the molecular processes that are associated with the S_N1 mechanism. These advances address issues relating to how the solvent mediates the dynamics of covalent bond formation as well as how the solvent controls the dynamics of ion pairs. These insights are linked to the development of new theoretical models for the electronic structure of the reacting system and the modulation of the electronic structure by solvent.¹¹ Molecular dynamic simulations have enhanced the sophistication of our understanding of these reaction processes.¹² With the recent advent in the formulation of new kinetic theories for how the solvent influences reaction processes, a whole new set of questions concerning the S_N1 mechanism comes to the forefront.¹³ Finally, time-resolved kinetic studies allow for a direct probe of the critical reactive intermediates found in the S_N1 reaction mechanism so that the questions raised by theory can now be addressed.¹⁴ It is the intent of this review to present these recent developments. However, before delving into this subject matter, a brief overview of the studies that led to our current understanding of the S_N1 mechanism will be presented.

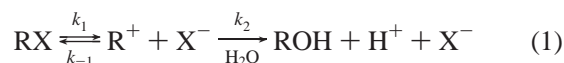
1. Introduction

The S_N1 reaction mechanism is fundamental to our understanding of numerous molecular processes found in organic chemistry. As such, the initial development of the mechanism is associated with such luminaries as Hughes, Ingold, Bartlett, Winstein, and Doering.^{1–7} This list does not even begin cover the major contributors to the field of carbonium ion chemistry, an intermediate central to the S_N1 mechanism.⁸

2. Background

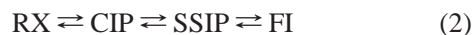
2.1. Formulation of the Intermediacy of Ion Pairs

In the initial development of the S_N1 mechanism during the 1930s, Hughes and Ingold proposed that the transition state for the rate-determining step in bond heterolysis, k_1 , involves partial charge separation in the transition state followed by dissociation into a pair of ions.^{1,2,15} The fate of the cation is governed by either reaction with the solvent, k_2 , leading to solvolysis product, or reaction with anion, k_{-1} , to re-form the reactant.



The formulation of this reaction scheme was based upon experiments examining the common ion effect and ionic strength effects.²

It was in 1954 that Winstein and co-workers observed an unusual effect in the rate enhancement of solvolysis of alkyl arenesulfonates upon the addition of lithium perchlorate in acetic acid.⁵ The rate of solvolysis was observed to increase to a greater extent than what would have been predicted by a normal ionic strength effect, and as a consequence, this phenomenon was termed the “special salt effect”.⁶ These studies led to the proposal that bond heterolysis leads to the initial formation of a contact ion pair (CIP), which upon further dissociation forms a solvent-separated ion pair (SSIP), followed by further separation to free ions (FI).



The special salt effect manifests itself in the ion-pair exchange of the solvent-separated ion pair with the lithium perchlorate that prevents the solvent-separated ion pair from returning to the contact ion pair and subsequent re-formation of the initial reactant, thus accelerating the rate of reaction. That this ion pair scheme is central to the S_N1 mechanism has been the subject of numerous investigations which have been thoroughly reviewed.⁹

2.2. Role of Solvent Participation in S_N1

Given the ionic nature of the transition state for reactions proceeding by the S_N1 mechanism, the polarity of the solvent should have a significant impact upon the kinetics of reaction for solvolysis. Seeking to define a parameter reflecting the ionizing power of the solvent, Grunwald and Winstein developed the Y scale derived from the kinetics of solvolysis for *tert*-butyl chloride in a variety of solvents.⁴ The Y scale is defined as

$$\log(k/k_0) = mY \quad (3)$$

where k_0 is the rate constant of solvolysis for 80% v/v ethanol/water, k is the rate constant for solvolysis in the solvent of interest, and m is the response of the reactant to the solvent ionizing power, where, by definition, $m = 1$ for *tert*-butyl chloride. The assumption behind this proposed relationship is that *tert*-butyl chloride reacts only by the S_N1 mechanism; that is, the participation of the solvent as a nucleophile in the rate-determining step of bond heterolysis does not occur.

Bentley and Schleyer have addressed the question as to whether the solvent participates as a nucleophile in the

solvolysis of *tert*-butyl chloride by correlating the rate of solvolysis of *tert*-butyl chloride with the rates of solvolysis of 1- and 2-adamantyl chloride, molecules for which back side attack of a nucleophile cannot occur.^{16–18} This correlation led to the conclusion that there is significant involvement of the solvent as a nucleophile in the solvolysis of *tert*-butyl chloride leading to a weak nucleophilically solvated ion pair yielding a stabilization through charge dispersal.

Employing a linear solvation energy relationship (LSER), Abraham, Taft, and Kamlet have argued against the Bentley and Schleyer proposal for nucleophilic solvent participation with *tert*-butyl chloride and instead have suggested that the hydrogen-bonding solvent serves to facilitate the rate of reaction through electrophilic assistance.¹⁹ As charge builds upon the leaving group in the transition state, the solvent forms a hydrogen bond with the leaving group serving to stabilize the complex. This proposed mechanism is based upon the correlation of the rate constant for heterolytic decomposition with three solvent parameters: the index for solvent dipolarity/polarizability, π^* , the ability of the solvent to form a hydrogen bond, α , and the propensity of the solvent to serve as a hydrogen bond acceptor, β . This latter term should correlate with the nucleophilic character of the solvent. The correlation of these three parameters with 15 solvents revealed that both π^* and α are dominant; the nucleophilic component β in the correlation made no contribution. This analysis reveals that the solvent serves to stabilize the developing charge distribution in the transition state through a bulk polarity effect as well as a specific interaction through hydrogen bonding of the solvent to the departing leaving group. This proposal received further substantiation by Farcasiu, Jahme, and Ruchardt in their study of the solvolysis for 1-adamantyl heptafluorobutyrate.²⁰

More recently, Gajewski re-examined the solvolysis data for *tert*-butyl chloride within the context of the KOMPH multiparameter equation.²¹ The functional form for the correlation includes the Kirkwood–Onsager formula for solvent polarity, the solvent cohesive energy density as defined by Hildebrand, and solvent hydrogen-bond donor and basicity parameters. The correlation revealed that solvent polarity, solvent cohesive energy density, and the propensity for hydrogen-bond donation to the leaving group are all important in governing the rate of solvolysis; nucleophilic assistance by the solvent is not involved in the rate-determining step for solvolysis.

However, Richard has recently suggested that it is not the participation of the solvent as a nucleophile leading to partial covalent bond formation between the solvent and the cation that serves to enhance the rate of reaction but rather the nucleophilic solvent serves to stabilize the transition state through electrostatic interaction with the developing positive charge.²² That the effect is greater in *tert*-butyl chloride than in 1-adamantyl chloride reflects the exclusion of solvent from the back side of the developing cation due to the molecular framework of the adamantyl system.

Finally, on the basis of electronic structure calculations, Martinez and co-workers have concluded that, for *tert*-butyl chloride solvolysis in water, a water molecule attacks in an S_N2 fashion on the back side of *tert*-butyl chloride, supporting the model suggested by Bentley and Schleyer.²³ It is noted that in these calculations a single water molecule and *tert*-butyl chloride are imbedded in a self-consistent reaction field model for bulk water; the bulk water was not treated at the quantum level.

As of 2007, it is clear that there is no general consensus as to the process by which the solvent participates in the solvolysis of *tert*-butyl chloride. To borrow a recent statement from Richard, "...the impression that studies of solvolysis at tertiary carbon have resulted in a morass of experimental data and which, when interpreted individually, provide support for conflicting mechanistic conclusions" captures the general sentiment of the field.²²

2.3. Nucleophilic Reactivities

Within the context of the Winstein model for the S_N1 reaction mechanism, a fundamental goal has been the characterization of the molecular parameters that govern nucleophilicity in cation–anion recombination reactions. During the 1970s and the 1980s, Ritchie's research program focused extensively on this issue.^{24–26} The rate constants for the reaction of numerous nucleophiles with a wide range of resonance-stabilized carbocations were examined. Normalizing the rate of reaction of a particular nucleophile, k_n , to the rate of reaction with water, k_{water} , the ratio was found to be independent of the identity of the cation, leading to the development of the N_+ scale.

$$\log(k_n/k_{\text{water}}) = N_+ \quad (4)$$

That the value of N_+ was independent of the cation was surprising. These observations led Ritchie to propose that the rate-determining step for the reaction of free ions to form a covalent bond must reside in the collapse of the solvent-separated ion pair (SSIP) to produce the contact ion pair (CIP).²⁴ Within the domain of highly resonance stabilized cations, the N_+ value for a given nucleophile is assumed to be associated with the energy for desolvation of the nucleophile allowing for the evolution of the SSIP into the CIP.

Mayr and co-workers have significantly expanded the range of nucleophile–electrophile combinations for the reactions of carbonium ions with a variety of nucleophiles, including alkenes, dienes, alkynes, enol ethers, arenes, amines, phosphates, and a number of anions.²⁷ Changing the definition of the normalization rate constant, $E_+ = \log k_{\text{water}}$, yields

$$\log k = s(E_+ + N_+) \quad (5)$$

where s is the slope of the correlation. Surprisingly, this most simple relationship gives an excellent correlation for this vast array of data. Why such a simple relationship encompasses such a wide range of reactivity has yet to be explained at the fundamental molecular level.

Building upon the laser flash photolysis studies of McClelland and Steenken, Mayr developed a quantitative free energy profile for the solvolysis of a variety of substituted benzhydryl chlorides in 80% aqueous ethanol and in trifluoroethanol.^{28,29} The assumed kinetic model is that of Hughes and Ingold given in eq 1, not the Winstein model given by eq 2. By individually determining each of the rate constants either through the kinetics of solvolysis or through the rate of reaction of the carbocations with the nucleophile X or water, the free energy profile is developed for eq 1.

A significant advance in our understanding of the lifetimes for carbocations and their reactivity with nucleophiles comes from the reaction "clocks" employed by Richard.^{10,30–33} On the basis of competition experiments between the nucleophile of interests and the azide anion with a known rate constant

for addition, thus serving as a clock, the absolute rate constants for nucleophilic addition are measured. Furthermore, for a molecular system such as 1-phenylethyl thiono-benzoate, the rate constant for the reorganization of the nucleophile within the ion pair is deduced as well as the rate constants for the reaction of water with the ion pair and with the free carbocation. In an attempt to understand the molecular parameters that ultimately control the rate of nucleophilic addition to the carbocation, Richards has undertaken a Marcus analysis of the rate constants that yields an intrinsic barrier for reaction, a methodology proposed by Albery.^{34–37} These studies represent the first attempt to apply Marcus theory in a comprehensive fashion to the reactions proceeding by the S_N1 mechanism. The utility of this approach will be discussed in the section on Marcus Theory.

3. Electronic Structure Theory for Bond Heterolysis

3.1. Early Theoretical Considerations

As the mechanistic features of bond heterolysis were beginning to be elucidated by experiment, principally through the work of Hughes and Ingold, simultaneously, theory was beginning to address the nature of the potential energy curves associated with these processes. The first theoretical model for bond heterolysis was development by Ogg and Polanyi in 1935.^{38,39} Today, their perspective would be identified as a valence-bond approach. They viewed the reaction surface as being composed of two valence-bond states: a homopolar covalent state and an ionic state. In the gas phase, the homopolar state gives rise to radical products that are lower in energy than the ion state dissociation products (Figure 1).

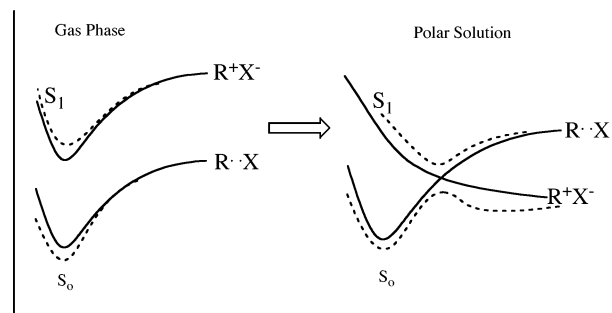


Figure 1. Potential energy surfaces for bond homolysis and heterolysis in the gas phase and in solution: solid curves, diabatic surfaces; dashed curves, adiabatic surfaces. Reprinted with permission from ref 97. Copyright 1996 American Chemical Society.

However, in the solution phase, the ionic state curve drops below the homopolar state at distances corresponding to product so that there is a crossing of the two states at a distance intermediate between reactant and product (Figure 1). At the point of crossing, a resonance interaction occurs between the two states, leading to a stabilization of the ground state surface. The point of the intersection of the two curves was identified as the transition state for reaction. By 1941, Polanyi and co-workers constructed quantitative potential energy diagrams for the dissociation of methyl iodide in water based upon a Morse function for the homopolar state and a Born model for the ionic state.³⁹ Ingeniously, the resonance interaction between the two states was derived from the dipole moment for methyl iodide. Evans extended the analysis to processes associated with primary, secondary, and tertiary halides.⁴⁰ That a tertiary

halide undergoes heterolysis more rapidly than a primary halide was shown to be due to the enhanced stability of the tertiary cation relative to the primary cation.

3.2. Valence-Bond Approach for Organic Reactivity

The use of valence-bond correlation diagrams to describe the origins of reactivity within the context of electronic structure was effectively reintroduced to the chemical community in the 1980s, principally through the work of Pross and Shaik, as well as Warshel.^{41–47} Their work builds upon the original formulation of Ogg and Polyani. Importantly, for bond heterolysis, Pross and Shaik expanded the model by incorporating solvent restructuring into the overall reaction coordinate.

From the perspective of anion–cation recombination where the ions are considered the reactants, the valence-bond configuration mixing diagram incorporates the influence of solvent.⁴³ The initial energy gap between the ionic surface $[(R^+(S_0) + X^-(S_0))]$ and the covalent surface $[(R\cdot(S_0) + X\cdot(S_0))]$ at the reactant configuration corresponds to the sum of the vertical ionization energy, $IP(X^-)$, and the electron affinity, $A(R^+)$; S_0 is the equilibrium solvent structure for the ion pair. As the reaction proceeds, the approach of the two ions is accompanied by the restructuring of the solvent so that the ion curve is destabilized with a concomitant stabilization of the covalent curve. The two curves eventually cross, leading to product formation with a solvent configuration S_1 , $[R-X(S_1)]$. At the crossing for some intermediate solvent configuration, S , there is a resonance interaction between the valence-bond states, β . Shaik has proposed that the crossing should be viewed “as a transformation that involves a single electron transfer switch which is synchronized to bond coupling”.⁴³ This continuous shift in electron density differs from a nonadiabatic electron-transfer process characterized by Marcus theory. Furthermore, at the transition state, the charge distribution is approximately constant, $R^{0.5+}X^{0.5-}$, and the resonance interaction β is assumed to be constant for a range of nucleophiles.

The free energy of activation, ΔG^\ddagger , for the formation of the covalent bond from the collapse of the ionic species is parametrized as follows:

$$\Delta G^\ddagger = f[IP[X^-(S_0)] - A[R^+(S_0)]] - \beta \quad (6)$$

where the crossing point corresponds to some fraction f of the combination of the IP and A . Examining Ritchie’s study of the combination reaction of the pyronin cation with a series of nucleophiles, Shaik found that the correlation of ΔG^\ddagger with the vertical ionization gave an excellent correlation.^{26,43} Furthermore, the Ritchie empirical N_+ scale for nucleophilicity was shown to be a function of the difference in the vertical ionization energies of the various nucleophiles.

3.3. Theoretical Studies of the Influence of Solvent on Bond Heterolysis

The first theoretical study to model bond heterolysis in *tert*-butyl chloride, which incorporates into the model both equilibrium and nonequilibrium solvation, was undertaken by Kim and Hynes in 1992.^{11,13} The model has since been extended to include *tert*-butyl bromide and *tert*-butyl iodide.^{48–50} The model involves the coupling of two gas-

phase diabatic surfaces, one purely covalent and one ionic, that interact with solvent polarization under equilibrium and nonequilibrium conditions to generate a two-dimensional adiabatic surface through a nonlinear Schrodinger formalism. The coordinates for the adiabatic surface are the bond stretch coordinate, r , and a collective solvent coordinate, s . The solvent is treated at the dielectric continuum level that separates the solvent electronic polarization, P_{el} , from the solvent orientational polarization, P_{or} . The diabatic surfaces are based upon a Morse potential for the covalent surface and a long-range Coulombic potential combined with a short-range Lennard-Jones potential obtained from the calculations of Jorgensen and Rossky.⁵¹

One of the fundamental questions addressed in this study is the form of the solvent coordinate at the point of the crossing of the two diabatic surfaces shown in Figure 1. If the electronic coupling β is small, Kim and Hynes have shown that in the solvent coordinate at the transition state there will be a barrier of the magnitude of $\Delta G_r/4$, where ΔG_r is the solvent reorganization energy; ΔG_r is directly analogous to that found in nonadiabatic electron transfer theory.¹¹ At the opposite limit of large electronic coupling, the barrier in the solvent coordinate goes to zero at the transition state. How one is to view the shift in charge as the system passes from the covalent surface onto the ionic surface at the transition will depend upon the magnitude of the electronic coupling.

The two-dimensional reaction coordinate for the heterolysis of *tert*-butyl chloride in acetonitrile places the reactant state at the bond distance 1.8 Å and the solvent configuration at $s = 0.05$; a value of $s = 0$ corresponds to the solvation structure of the purely covalent state, and a value of $s = 1$ corresponds to the solvation structure of the purely ionic state.¹¹ The saddle point on the reaction surface, corresponding to the transition state, occurs 28 kcal/mol above the reactant, a value in excellent agreement with experiment, and the bond lengthens to 2.47 Å.⁵² The coefficient of the contribution of the ionic state to the wave function at the transition state is $c_1^2 = 0.61$, which can be viewed as the wave function having a 61% ionic character. This contrasts with the standard VB model that does not allow the solvent to adjust to the electronic structure of the wave function, leading to a constant contribution of 50% for the ionic state at the transition state. The electronic coupling at the transition state is large, $\beta = 17.7$ kcal/mol. With this large electronic coupling between the two diabatic states at the transition state, the two-dimensional reaction surface reveals no barrier in the solvent coordinate at the transition state. As the system passes through the transition state, there is a smooth evolution in the charge distribution; there is no discontinuity in the charge distribution at the transition state that would normally be associated with an electron-transfer process. This observation is congruent with that of Shaik.⁴³ As the bond dissociates, the movement of the electron onto the leaving group should be viewed as a gradual shift, not an electron hop.

The nature of the dielectric-continuum model is such that the reaction of *tert*-butyl chloride can be examined in nonpolar solvents such as chlorobenzene and even benzene.¹¹ The position of the transition state increases to 2.53 Å in chlorobenzene and increases even further to 2.75 Å in benzene. Interestingly, the charge character of the transition state increases as the solvent polarity decreases, for the wave function is 67% ionic in chlorobenzene and 89% ionic in benzene, an observation that at first glance is counter to

intuition. However, Kim and Hynes have rationalized these findings within the context of the Hammond Postulate.¹¹

As the solvent polarity increases, the free energy of activation for bond heterolysis decreases: $\Delta G^\ddagger = 32.7$ kcal/mol in benzene, $\Delta G^\ddagger = 30.0$ kcal/mol in chlorobenzene, and $\Delta G^\ddagger = 28.0$ kcal/mol in acetonitrile. Ingold has argued that the reduction in the ΔG^\ddagger with an increase in solvent polarity for bond heterolysis is due to the enhanced stabilization of the ionic structure with an increase in polarity.^{15,53} However, Kim and Hynes have examined the solvation energy of the ionic structure at the transition state and have found that it actually decreases as the solvent polarity increases. This is attributed to the reduction of ionic character in the transition state with an increase of solvent polarity: 89% ionic in benzene, 67% ionic in chlorobenzene, and 61% ionic in acetonitrile. The source of the decrease in the free energy of activation with an increase in solvent polarity comes from the distance dependence of the electronic coupling, $\beta(r)$. As the solvent polarity increases, the crossing of the ionic surface with the covalent surface occurs at a shorter distance (Figure 2). In the vicinity of these crossings, the value of β increases

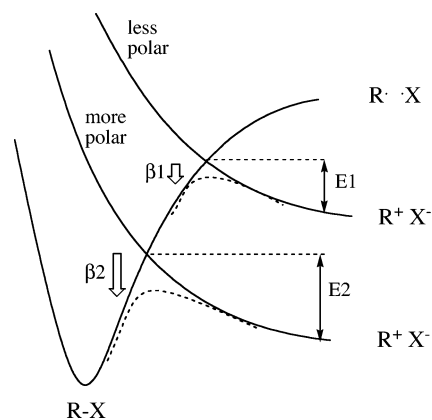


Figure 2. Reaction diagram for bond heterolysis of *tert*-butyl chloride as a function of solvent polarity. On increasing solvent polarity, the electronic coupling between the two diabatic surfaces (solid curve) increases, i.e., $\beta_2 > \beta_1$. Reprinted with permission from ref 101. Copyright 2005 American Chemical Society.

in a strongly nonlinear fashion as the distance decreases due to the significant increase in the overlap between the ionic and covalent states. Thus, the electronic coupling between the two diabatic surfaces is much greater in acetonitrile as compared to that in benzene: $\beta_2 > \beta_1$ (Figure 2). This enhanced coupling is what gives rise to the reduction in the free energy of activation for bond heterolysis, not the increase in the solvation energy of the transition state as suggested by Ingold.⁵³

Finally, the characteristics of the passage through the transition state for *tert*-butyl iodide are more complicated when compared to those of *tert*-butyl chloride and *tert*-butyl bromide because in the region of the transition state there is a barrier in the solvent coordinate for the iodide that is not found for chloride and bromide.^{48,49} The origin of the solvent barrier can be traced to the weak electronic coupling of the two diabatic states in the transition state for the iodide as $\beta = 4.1$ kcal/mol compared to $\beta = 17.7$ kcal/mol for the chloride and $\beta = 13.9$ kcal/mol for the bromide. Since the molecular processes associated with bond heterolysis in the transition state include both bond elongation and thermally activated solvent reorganization, a multidimensional dynamic model for this molecular process becomes much more

complicated than the model appropriate for bond heterolysis for the chloride and bromide where there is no barrier in the solvent coordinate at the transition state. Hynes and co-workers have examined various models to describe the molecular processes found in bond heterolysis for *tert*-butyl iodide, but the scope of the discussion is sufficiently complex that the reader is referred to the original exposition.⁵⁰

3.4. Empirical Valence-Bond Model with Explicit Solvent Interaction

A very novel application of the empirical valence-bond model (EVB) that explicitly incorporates a molecular model for the solvent is the recent study by Rossky and co-workers of the effect of supercritical water on *tert*-butyl chloride bond heterolysis.^{54,55} The properties of supercritical water and the influence that it has on governing organic reactivity have been the subject of numerous investigations.^{56,57} Above the critical temperature of water ($T_c = 647.15$ K), the density can be changed over a great range at constant temperature by small changes in pressure. Accompanying the reduction in density is a dramatic decrease in the dielectric constant of water that approaches values normally associated with organic solvents. A question central to the S_N1 mechanism is, under what conditions can the dominant dissociation pathway switch from bond heterolysis to bond homolysis?

In a molecular dynamic simulation employing a two-state EVB model that interacts with 500 water solvent molecules through a combination of electrostatics and a Lennard-Jones potential, the ionic nature of the bond dissociation process for *tert*-butyl chloride in a range of solvent densities, 1–0.0435 g cm⁻³, was characterized.⁵⁵ Under ambient conditions, the model predicted a barrier height of 23 kcal/mol, which is in good agreement with the experimental value of 19.5 kcal/mol, and the transition state is located at 2.35 Å in the bond stretch coordinate.⁵² The contact ion pair is found at 3.1 Å, and the barrier for collapse of the contact ion pair to re-form the bond is 7 kcal/mol, a value very close to the estimate derived from experiment by Abraham.⁵² Under supercritical conditions, dissociation to contact ion pairs is observed for densities as low as 0.29 g cm⁻³, which corresponds to a dielectric constant of $\epsilon = 5.4$. When the density is further reduced to 0.0435 g cm⁻³, leading to a further reduction in the dielectric constant to a value of $\epsilon = 1.5$, the shallow well associated with the contact ion pair disappears. However, the nature of the wave function at these extended distances, > 2.5 Å, is totally ionic; homolytic bond dissociation does not occur even at these low dielectric constants, which is the key finding of the study.

Following the theoretical methodologies of Rossky and co-workers, Winter and Benjamin examined the molecular dynamics for the ionic dissociation of *tert*-butyl chloride at the water/carbon tetrachloride interface, leading to the derivation of the potential of mean force for dissociation as a function of position relative to the interface.⁵⁸ As the substrate moves from the interface into the organic layer, the transition state for dissociation moves to longer distances and increases in energy. At distances greater than 3 Å from the interface, the minimum attributed to the contact ion pair disappears. The dynamic roughness at the interface surface is found to enhance the ionic dissociation process.

3.5. Quantum Calculations

There have been several quantum calculations at the semiempirical and higher levels that examined the reaction

coordinate for *tert*-butyl chloride bond heterolysis in water.^{59–62} The water is incorporated into the model either through molecular mechanics or explicitly at the quantum level. For the explicit consideration of water at the quantum level, clusters up to the size of 14 were considered. Employing DFT at the RB3LYP/6-31G* level, Yamabe and Tsuchida examined the *tert*-butyl cation symmetrically solvated by up to $n = 14$ water clusters.⁶¹ The planar *tert*-butyl cation was found to reside at a saddle point, as evidenced by the one imaginary frequency for the complex, leading to the conclusion that, in water, it does not exist as a stable species, a finding that would surprise general consensus.²¹ Examining the heterolysis of *tert*-butyl chloride in water clusters varying between $n = 6$ and $n = 14$, they found that as the chloride anion departs, there is a synchronous back side attack on the *tert*-butyl moiety by water. The reaction is facilitated by a bridge of four water molecules that link via a hydrogen-bonded network from the departing chloride to the water molecule undergoing back side attack. As the water attacks at the backside, there is a concomitant proton transfer to the nearest neighboring water leading to the formation of *tert*-butanol. Interestingly, the departure of the chloride ion does not occur along the C_{3v} axis of the *tert*-butyl group but instead occurs perpendicular to the axis, allowing a front side water molecule to synchronously move into the chloride's original position. That water is acting as both a nucleophile and an electrophile is contrary to most experimental studies employing linear solvation energy relationships analysis.^{19,21}

The conclusion from the Yamabe–Tsuchida study is that heterolysis of *tert*-butyl chloride in water involves a synchronous displacement of chloride and attack by water facilitated by a hydrogen-bonded network of four water molecules.⁶¹ In this system of up to 14 water molecules, the commonly perceived contact ion pair of the *tert*-butyl cation and chloride anion does not exist, an observation at odds with quantum calculations that treat the bulk water at the level of molecular mechanics.⁵⁵ Whether this model persists as the number of solvating water molecules increases and if this is unique to water remain to be addressed.

4. Kinetic Theories

4.1. Transition-State Theory

The effect of solvent upon the rates of the reactions associated with the S_N1 mechanism traditionally has been viewed within the context of transition-state theory (TST).^{63–67} Developed in the 1930s, the central tenants of TST are twofold: the reactant and the activated complex are in thermodynamic equilibrium, and once the activated complex passes into the region of the transition state, the system evolves directly into product with no recrossing of the transition state. With these two assumptions and the machinery of statistical mechanics to treat the equilibrium between the reactant and the activated complex, the rate expression is derived whose ingredients include the partition functions for the reactants, Q_R , and the transition state, Q_{TST} , as well as the energy separation between the zero-point energy of the reactant and the transition state, E_0 .

$$k_{TST} = \frac{k_B T}{h} \frac{Q_{TST}}{Q_R} \exp(-E_0/k_B T) \quad (7)$$

The partition function Q_{TST} has one less degree of freedom

relative to Q_R , resulting from the conversion of one vibrational degree of freedom from the reactant into the reaction coordinate associated with translation through the transition state.

At the time of the formulation of transition-state theory, it was recognized that the activated complex could, in principle, undergo multiple recrossings of the transition state, thus reducing the rate of reaction.⁶³ That the solvent could effect multiple recrossings was not pursued in the original formulation, and for most reactions the recrossing parameter κ , discussed by Eyring, is set to unity.⁶³

Although the solvent influence upon the dynamics of the passage through the transition state was not initially addressed, it was recognized that solvent could have a major effect upon the rate of reaction compared to the gas-phase value as a result of the differential solvation of the reactants and the transition state.^{68–70} This influence is manifested in the potential of mean force as reflected in E_0 . Since the pioneering mechanistic studies of Hughes and Ingold, the concept of the solvent effect upon the rate of reactions has been discussed normally within the context of the dependence of E_0 on the medium.

4.2. Kramers Theory

In 1940, Kramers extended transition-state theory by addressing the question of the control that a solvent will have upon inducing multiple recrossings of the transition state prior to product formation.^{66,71} The theoretical perspective taken was within the context of the stochastic Langevin equation for the escape of a Brownian particle of effective mass μ over a one-dimensional barrier U :

$$\mu \ddot{x} = -\frac{\delta U}{\delta x} - \mu \zeta \dot{x} + R \quad (8)$$

where the net force on the particle is $\mu \ddot{x}$ and is a function of $\delta U/\delta x$, the force due to the potential of mean force at the transition state, $\mu \zeta \dot{x}$, the frictional term associated with the movement of the particle through the solvent, R , a random force upon the particle due to the solvent, and ζ , the friction coefficient due to the interaction of the particle with the solvent. The resulting rate expression takes the form

$$k = k_{TST} \kappa_{KR} \quad (9)$$

$$\kappa_{KR} = [1 + (\zeta/2\omega_b)^2]^{1/2} - (\zeta/2\omega_b)$$

where k_{TST} is the rate constant from transition-state theory. The frequency of the potential of mean force U at the transition state is ω_b and is the term that is responsible for driving the system off of the transition state toward product. κ_{KR} can be viewed as the correction to transition-state theory due to the influence of the solvent on the diffusional motion through the transition state.

The effect of the solvent on the dynamics of the passage through the transition state is controlled by the term $\zeta/2\omega_b$. If the magnitude of the friction ζ is small relative to the reaction barrier frequency ω_b , i.e., $\zeta/2\omega_b \ll 1$, then the correction κ_{KR} approaches 1 and the rate constant approaches k_{TST} . However, if the solvent friction ζ is large relative to ω_b , i.e., $\zeta/2\omega_b \gg 1$, then κ_{KR} approaches $\zeta/2\omega_b$, and the solvent controls the diffusional passage of the system through the transition state, which can significantly reduce the rate constant for reaction below the transition state value k_{TST} .

4.3. Grote–Hynes Theory

The next significant advance in our understanding of how the solvent controls the dynamics of transition state passage is due to the work of Grote and Hynes in the early 1980s.^{72,73} They recognized that if the passage of the system through the transition state is slow relative to the solvent's response, then the effect of the solvent would indeed be characterized by the time independent friction term ζ found in Kramers theory. However, if the passage through the transition state is comparable to or faster than the solvent response, then a time independent ζ is not the appropriate measure of the solvent's influence. These considerations led Grote and Hynes to pursue the problem of transition state passage within the context of the generalized Langevin equation.

The generalized Langevin equation takes the form

$$\mu\ddot{x}(t) = -\frac{\delta U}{\delta x} - \mu \int_0^t d\tau \zeta(\tau) \dot{x}(t-\tau) + R(t) \quad (10)$$

where the terms have the same definitions as in eq 8, except that \ddot{x} , ζ , and R are now time dependent functions.⁷² The time dependent friction coefficient $\zeta(t)$ is related to the time correlation function of the fluctuating forces of the solvent $R(t)$ on μ through the relationship

$$\zeta(t) = (1/\mu k_B T) \langle RR(t) \rangle \quad (11)$$

The rate constant given by Grote–Hynes, k_{GH} , is

$$k_{GH} = k_{TST}(\lambda_r/\omega_b) \quad (12)$$

with k_{TST} reformulated as

$$k_{TST} = (\omega_R/2\pi) \exp(-E_0/RT) \quad (13)$$

where ω_b is the frequency at the barrier top and ω_R is the frequency in the reactant well. The term λ_r is the actual reactive frequency defined as

$$\lambda_r = \omega_b^2 / (\lambda_r + \zeta(\lambda_r)/\mu) \quad (14)$$

where $\zeta(\lambda_r)$ is the Laplace transform of the time dependent friction expressed as

$$\zeta(\lambda_r) = \int_0^\infty dt \zeta(t) \exp(-\lambda_r t) \quad (15)$$

The Grote–Hynes model significantly modifies the Kramers perspective on the basis of how strong the solvent influence will be in inducing multiple recrossings of the transition state. In the limit of a high reaction barrier frequency, ω_b , the time scale for residence in the transition state will be short compared to the time scale for the sum total of the solvent fluctuations through translation and rotation that contribute to the generation of the friction ζ . The net effect is a reduction in the solvent friction experienced by transiting species relative to the situation where passage over a low barrier frequency ω_b increases the time scale for residence in the transition state, which allows for the full development of the friction ζ . Thus, passage over a barrier with a high frequency ω_b will experience significantly

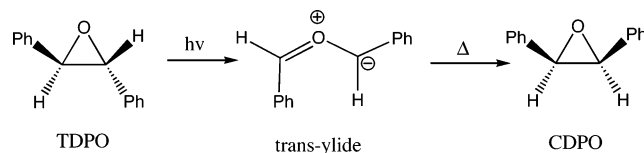
fewer recrossings compared to passage over a barrier with a low frequency ω_b . As ω_b increases, k_{GH} approaches k_{TST} .

4.4. Large Amplitude Motions—A Test of Hydrodynamic Theories

During the 1980s and early 1990s, numerous studies appeared examining the applicability of the Kramers model and the Grote–Hynes model for interpreting the solvent's influence upon the dynamics of isomerization for *trans*-stilbene and other polyenes.^{74–79} These studies have been reviewed by Waldeck in 1991.⁸⁰ Only the conclusions pertinent to the reaction processes associated with the S_N1 mechanism will be presented.

There are two central issues surrounding the application of the Kramers model to the transition state dynamics for isomerization.⁸⁰ The first issue is whether the reaction coordinate can be viewed as one-dimensional, a fundamental assumption inherent in the formulation of the Langevin equation, or whether the reaction coordinate is inherently multidimensional. The second issue is how to model the friction coefficient ζ . In the initial studies for the isomerization of *trans*-stilbene, the friction coefficient was assumed to be proportional to the zero-frequency solvent shear viscosity, η_s , based on the Debye–Stokes–Einstein relationship, $\zeta \propto \eta_s$. This assumption led to a poor fit of the Kramers model to the experimental data, suggesting that the macroscopic shear viscosity is inappropriate for the description of the friction felt by the molecule in the transition state. Improved fits were obtained when the friction was related to the viscosity associated with the molecular rotation–reorientation times.⁷⁸ Finally, Saltiel and co-workers developed a model for the friction in terms of a microviscosity obtained from the translational diffusion coefficients of toluene in *n*-alkane solvents.⁸¹ They found that the Kramers model gave an excellent fit to the kinetics of isomerization of *trans*-stilbene.

In the stilbene experiments, the reaction barrier heights are small, ~ 3 kcal/mol, which should lead to a low barrier frequency ω_b that places the system in a regime where the Kramers model should be valid for large frictions. The question becomes for reactions with larger barriers, ~ 9 kcal/mol, where the barrier frequency ω_b should be much greater than that for *trans*-stilbene, does the Kramers model still work? In our study of the dynamics associated with the orbital symmetry controlled ring closure of the *trans*-ylide, produced upon irradiation of *trans*-2,3-diphenyloxirane (TDPO), to form *cis*-2,3-diphenyloxirane (CDPO), we found that the Kramers model cannot account for the kinetic data whether the friction coefficient is modeled as a shear viscosity or even as a microviscosity.⁸² However, employing



Grote–Hynes theory, where the time dependent friction was modeled within the frequency dependent hydrodynamic model developed by Bagchi and Oxtoby, we found that Grote–Hynes theory gave a superior, although not perfect, fit of the experimental data.^{72,83} The derived barrier for this reaction is of the order of 9 kcal/mol in *n*-alkane solvents. That Grote–Hynes theory gave less than a perfect fit to the

data could be the result of the simplifying assumptions in the modeling of the frequency dependence of the friction.⁸³ However, it is also possible that the reaction coordinate is not truly one-dimensional.⁸⁰

4.5. Grote–Hynes Theory for Unimolecular Ionic Dissociation

The heterolytic dissociation process that is central in the S_N1 mechanism clearly must involve substantial solvent reorganization as the system passes through the transition state. Hynes and co-workers have addressed the nature of this coupling within the context of Grote–Hynes theory.^{84–86} The reaction is modeled as the passage of a charge species over a parabolic reaction barrier with an associated frequency ω_b . The time dependence of the friction $\zeta(t)$ is modeled as a charge interacting with a dielectric continuum whose time dependence takes the form of the Debye model for $\epsilon(t)$, a time dependent dielectric constant. From the results of the analysis, the critical time scale associated with solvent motion is the solvent longitudinal relaxation time τ_1 , defined as $\tau_1 = \epsilon_\infty \tau_D / \epsilon_0$, where ϵ_∞ and ϵ_0 are the high-frequency and static dielectric constants and τ_D is the Debye relaxation time for the solvent. Also associated with the interaction of the charge with the solvent is a harmonic restoring potential with an associated solvent frequency ω_s . This force resists the motion of the charged particle off of the transition state. The frequencies ω_s and ω_b are opposite in sign.

The nature of the dynamical processes associated with passage through the transition state depends on the relative magnitudes of solvent frequency $|\omega_s|$ and reaction barrier frequency $|\omega_b|$.⁸⁴ If $|\omega_s| > |\omega_b|$, the charged particle is entrained in the transition state undergoing multiple oscillations until the solvent undergoes a fluctuation on the time scale τ_1 allowing the charged particle to move off of the transition state. For a given barrier frequency, ω_b , as the time scale of the solvent relaxation τ_1 increases, the transmission coefficient κ_{GH} , defined as $\kappa_{GH} = k_{GH}/k_{TST}$, decreases (Figure 3). However, in the regime where $|\omega_s| < |\omega_b|$, as τ_1 increases, there is only a small decrease in κ_{GH} (Figure 3).

This behavior can be understood within the context of an effective potential, ω_{eff} , which is a function of ω_s and ω_b , where $\omega_{eff}^2 = -\omega_b^2 + \omega_s^2$. In the limit $|\omega_s| > |\omega_b|$ and thus

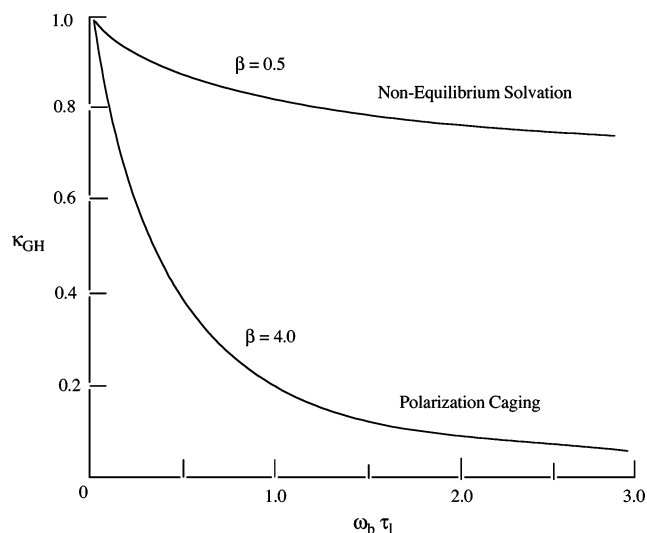


Figure 3. Dynamical transmission coefficient, $\kappa_{GH} = k_{GH}/k_{TST}$, for values of $\beta = 0.5$ and $\beta = 4.0$ as a function of the reduced solvent relaxation time, $\omega_b \tau_1$. $\beta = |\omega_s|/|\omega_b|$.

$\omega_{eff}^2 > 0$, the system finds itself trapped in an effective potential dominated by the solvent preventing movement off of the transition state, resulting in multiple recrossings; it is only when the solvent relaxes with time τ_1 that the system evolves into product (Figure 4).⁸⁴ Clearly, as τ_1 increases,

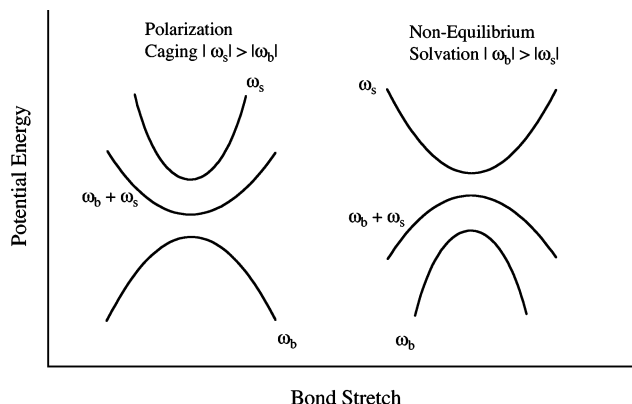


Figure 4. Schematic illustration of the interplay between the reaction barrier frequency, ω_b , and the solvent frequency, ω_s . Polarization caging: $|\omega_s| > |\omega_b|$. Nonequilibrium solvation: $|\omega_b| > |\omega_s|$.

the number of recrossings increases, thus increasing the deviation from the prediction of transition-state theory; this effect can be large, as deviations from the predictions of transition-state theory can exceed an order of magnitude (Figure 3). This limit is defined as the polarization-caging regime. At the other limit, $|\omega_s| < |\omega_b|$ and thus $\omega_{eff}^2 < 0$, the system can evolve toward product without the necessity of solvent rearrangement (Figure 4). The effect of the solvent is to exert a drag on the motion through the transition state; the deviations from the predictions of transition-state theory are not as large (Figure 3). This limit is defined as the nonequilibrium solvation limit, as solvent reorganization is not required for the system to move off of the transition state; the solvent only retards the motion off of the transition state.

4.6. Nonequilibrium Solvation in *tert*-Butyl Chloride Heterolysis

On the basis of a nonlinear Schrodinger formulation for the coupling of the solute electronic structure with the solvent, Kim and Hynes examined the reaction pathway for *tert*-butyl chloride heterolysis as a function of solvent dielectric.¹³ Two reaction pathways were examined. The first corresponds to conventional transition-state theory based on the assumption that the solvent maintains equilibrium solvation throughout the entire reaction trajectory; this pathway is identified as the equilibrium solvation path (ESP). To maintain equilibrium solvation, as the system passes through the transition state, the solvent is continuously changing in the s coordinate to accommodate the shift in charge distribution upon elongation in the bond length r . The response of the solvent to the motion in r is instantaneous. Thus, passage through the transition state under the constraints placed by the ESP leads to simultaneous changes in both r and s .

The second reaction pathway is identified as the solution reaction pathway (SRP). This is the intrinsic reaction pathway developed by Lee and Hynes for condensed phase reactions that was based upon the work of Fukui for gas-phase reactions.^{87,88} This is the minimum free energy pathway that allows for the solvent to be out of equilibrium along the reaction coordinate. For *tert*-butyl chloride in acetonitrile,

the SRP reaction coordinate involves an initial solvent fluctuation about the system that initiates bond heterolysis. As the system passes through the transition state, the direction of motion is along the bond stretch coordinate r while there is no change in the solvent coordinate s ; the solvent is frozen as the system moves through the transition state, leading to nonequilibrium solvation. This picture is diametrically opposed to the basic assumptions of transition-state theory.

The breakdown in the predictions of transition-state theory is reflected in the derived value of κ . On the basis of analysis within the context of Grote–Hynes theory, $\kappa = 0.65$ for the solvent acetonitrile.¹³ The effect of the frozen solvent configuration as the system traverses the transition state is to exert a drag on the molecular system reducing the rate of passage through the transition state below the prediction of transition-state theory. For the potential developed for *tert*-butyl chloride heterolysis, the curvature of the reaction barrier is rather sharp with a frequency of $\omega_b \sim 70 \text{ ps}^{-1}$ while the frequency associated with the solvent at the transition state is much smaller, $\omega_s = 15 \text{ ps}^{-1}$. Thus, the system can pass through the transition state without the rearrangement of the solvent, conditions for nonequilibrium solvation.

The molecular dynamic simulation by Wilson and Hynes for the bond heterolysis of *tert*-butyl chloride in water supports the above picture, as the κ value derived from simulation is $\kappa_{\text{MD}} = 0.53$.¹² If this reaction were to be viewed within the context of Kramers theory, the theoretically predicted value is $\kappa_{\text{KR}} = 0.019$, while if the reaction were to be viewed within the context of Grote–Hynes theory, the theoretically predicted value is $\kappa_{\text{GH}} = 0.58$, which more accurately describes the computer modeling. The discrepancy in the predictions of Kramer’s theory relative to simulation values for κ points toward the importance of viewing the process within the context of a frequency dependent friction.

5. Theoretical Perspective on Ion Pair Interconversions

Jorgensen and Rossky were the first to develop the free energy surface for the interconversion of the contact ion pair and the solvent-separated ion pair for *tert*-butyl chloride in water.⁵¹ Their Monte Carlo simulations employed a model for the *tert*-butyl cation and the chloride anion embedded in 250 water molecules. The calculations revealed a well-defined energy minimum for the contact ion pair with an anion–cation separation of 2.9 Å. A second minimum at 5.75 Å was also observed; this latter minimum is rather broad, and a clear energetic distinction between solvent-separated ion pair and free ions was not ascertained. The energy of the contact ion pair is 4 kcal/mol above the solvent-separated pair and 2.1 kcal/mol above the free ions. This latter value compares well with Abrahams’ experimentally derived value for the separation of *tert*-butyl chloride in water to free ions.⁵² Finally, the barrier for the contact ion pair conversion to the solvent-separated ion pair is rather small, on the order of 2 kcal/mol.

The nature of the passage through the transition state for the conversion of a contact ion pair into a solvent-separated ion pair for reactions proceeding by the S_N1 mechanism has not been addressed theoretically. Thus, we turn to model studies for the dynamics of ion pair interconversion to gain insight into the nature of this process.^{89,90} The central question in this regard is whether transition-state theory, which does not explicitly incorporate the dynamical character of the solvent into the formulation, is a proper description for ion

pair interconversion. In 1990, Hynes and collaborators undertook a molecular dynamics simulation for the conversion between contact and solvent-separated ion pairs.⁹⁰ The ions were modeled as spherical charges, and the solvent was modeled as an 2 Å entity with a dipole moment of either 2.4 or 3.0 D. The model potential of mean force placed the contact ion pair 16 kcal/mol below the solvent-separated ion pair. The barrier for CIP → SSIP is 17.6 kcal/mol while the barrier for SSIP → CIP is 1.5 kcal/mol for a solvent with a dipole moment of 2.4 D. From the MD simulations, the κ factor measuring the deviations from the prediction of transition-state theory is $\kappa = 0.18$. Both the Kramer’s model and the Grote–Hynes model gave a good account of the transmission coefficient. However, examining the individual trajectories, the source of the deviation from transition-state theory comes from multiple recrossings of the barrier prior to reaction. The Kramer’s model portrays the passage as a simple overdamped diffusional process through the transition state governed by the time independent friction coefficient ζ . In the Grote–Hynes model, the transient is trapped in a polarization cage, leading to multiple recrossings of the transition state prior to solvent relaxation. Thus, the transmission coefficient for ion pair interconversion is determined by the solvent dynamics. The dynamics derived from the MD simulations are more accurately described by the Grote–Hynes model than by the Kramers model. In subsequent MD simulations of the dynamics of ion pair interconversion for sodium chloride in a variety of solvents, Grote–Hynes theory is found to give an accurate rendering of the transmission coefficients.⁹¹

6. Experimental Studies for the S_N1 Mechanism

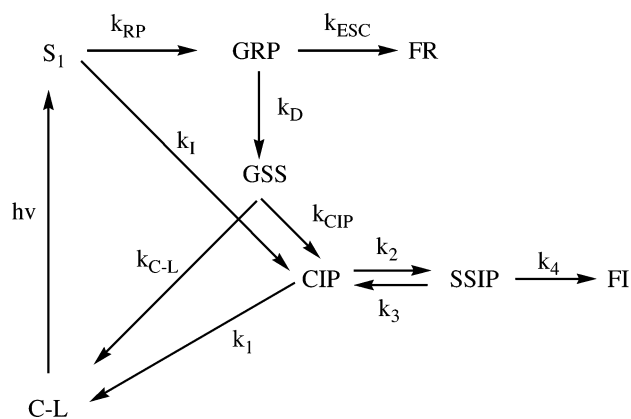
6.1. Kinetic Studies for Benzhydryl Derivatives

For the sake of comparison with theoretical investigations that examine the mechanism of bond heterolysis, *tert*-butyl chloride would have been the molecule of choice for time-resolved kinetic studies. However, the absorption spectrum associated with the *tert*-butyl cation has not been experimentally characterized.⁹² Thus, it is derivatives of benzhydryl [(C₆H₅)₂C-L] that have been employed most extensively in time-resolved kinetic studies. The optical properties of the intermediates encountered in the reaction pathways have been well characterized. Steenken and McClelland have shown that the variously substituted benzhydryl radicals absorb in the region 330–350 nm with large extinction coefficients, of the order of $\log \epsilon = 4.5 \text{ M}^{-1} \text{ cm}^{-1}$.^{29,93} Derivatives of the benzhydryl cation absorb between 430 and 530 nm, again with large extinction coefficients, of the order of $\log \epsilon = 5 \text{ M}^{-1} \text{ cm}^{-1}$. Consequently, the two intermediates produced in photochemical studies are spectroscopically well resolved. Furthermore, employing 3-methoxy substitution, the quantum yield for cation formation is large, a manifestation of the “meta effect” first enunciated by Zimmerman in the 1960s.⁹⁴

In 1994, we began a series of studies into the photochemical processes associated with bond homolysis and bond heterolysis for benzhydryl chloride in acetonitrile employing both femtosecond and picosecond laser technologies.^{14,95–101} These studies in the ensuing 5 years led to the formulation of the reaction scheme shown in Scheme 1.

The 266 nm irradiation of benzhydryl chloride (C-L) in acetonitrile places the system on the potential energy surface associated with the first excited singlet state (S₁). The predominate decay pathway for S₁ is the partitioning between

Scheme 1



bond homolysis, giving rise to the geminate radical pair (GRP), and bond heterolysis, giving rise to the contact ion pair (CIP). The initial production of the GRP in acetonitrile occurs with an apparent rate constant $k_{RP} = 2.9 \times 10^{12} \text{ s}^{-1}$ while the initial production of the CIP occurs with a rate constant $k_1 = 1.2 \times 10^{12} \text{ s}^{-1}$.⁹⁸ The nature of the potential energy surfaces associated with the partitioning of S_1 between the formation of the GRP and the CIP is assumed to involve the participation of conical intersections, although this has not been formally characterized. The GRP subsequently decays by two pathways. The first is separation to free radicals, k_{ESC} , occurring on a time scale of 140 ps in acetonitrile, and the decay onto the ground state surface, k_D , occurring on a time scale of 190 ps, which then partitions between re-formation of the initial product, k_{C-L} , and CIP formation, k_{CIP} . The rate constants associated with the latter two processes have not been resolved. An interesting feature associated with the GRP decay onto the ground state surface is that the kinetics associated with these processes are time dependent.⁹⁸ This may reflect internal restructuring within the radical pair prior to the transition onto the ground state surface. The exact nature of the transition has not been fully elucidated, but in a related molecular system, 3-methoxybenzyl acetate, Pincock has suggested that this internal conversion be viewed as nonadiabatic electron-transfer characterized by Marcus electron transfer theory.^{102–104}

The fate of the ion pairs is deduced from the triphasic decay of the cation signal monitored at 440 nm.¹⁴ Casting the decay processes within the context of the Winstein model for ion pair interconversions, eq 2, the rate constants for collapse of the CIP to form a covalent bond, k_1 , the separation of the CIP into the SSIP, k_2 , the collapse of the SSIP back to the CIP, k_3 , and the further separation of the SSIP into free ions (FI), k_4 , are resolved for benzhydryl chloride in acetonitrile (Scheme 1). The corresponding rate constants for a variety of benzhydryl derivatives are given in Table 1.¹⁰¹

6.2. Role of Polarization Caging in the Collapse of the CIP

Prior to our experimental study of benzhydryl chloride, the role of polarization caging versus nonequilibrium solvation in covalent bond formation had not been addressed from an experimental perspective. To assess in which domain the reaction dynamics occur, it is necessary to establish the degree to which the time scale associated with passage through the transition state deviates from the prediction of transition-state theory. Since the rate constant k_{TST} associated

Table 1. Kinetic Parameters for Ion Pair Dynamics for Benzhydryl Chloride (BC), Benzhydryl Bromide (BB), 3,4-Dimethoxybenzhydryl Acetate (MethoxyD+), 3-Methoxy-4'-methylbenzhydryl Acetate (MethylD+) and 3-Methoxybenzhydryl Acetate in Acetonitrile at 23 °C^a

compound	k_1^b ($\times 10^9 \text{ s}^{-1}$)	k_2 ($\times 10^9 \text{ s}^{-1}$)	k_3 ($\times 10^9 \text{ s}^{-1}$)	k_4 ($\times 10^9 \text{ s}^{-1}$)
BC	3.8	2.9	0.13	0.78
BB	3.2	5.6	<i>c</i>	<i>c</i>
MethoxyD+	0.6	1.3	0.39	0.80
MethylD+	2.2	3.0	0.39	0.80
D+	3.0	3.5	0.40	0.80

^a Rate constants from Scheme 1 and ref 101. ^b Uncertainties in fits $\pm 10\%$. ^c Cannot be resolved.

with transition-state theory is only a hypothetical quantity, it is a quantity that can only be derived from its theoretical formulation. One such formulation has been given by Kim and Hynes.¹³

$$k_{TST} = \left(\frac{\omega^R}{2\pi} \right) \left(\frac{\omega_S(R)}{\omega_S(r^\ddagger)} \right) \left(\frac{Q_{rot}(r^\ddagger)}{Q_{rot}(R)} \right) \exp(-\Delta G^\ddagger/k_b T) \quad (16)$$

The vibration frequency ω^R is that associated with the contact ion pair that leads to its collapse and is modeled after the vibrational frequencies associated with alkali ion contact ion pairs.⁹⁵ Q_{rot} is the rotational partition function for the reactant R and the transition state r^\ddagger which again is estimated on the basis of the assumed structures for the CIP and for the transition state. ΔG^\ddagger is the free energy difference between the CIP and the transition state. The ratio of the solvent frequencies $\omega_S(R)/\omega_S(r^\ddagger)$ associated with the CIP and the transition state has yet to be determined experimentally, and thus, we rely on the values obtained theoretically for *tert*-butyl chloride in acetonitrile, $\omega_S(R)/\omega_S(r^\ddagger) = 1.5$.¹³ On the basis of these estimated values, the transition-state theory rate constant for the collapse of the CIP giving rise to a carbon–chlorine covalent bond in benzhydryl chloride is given by

$$k_{TST} = (5.7 \times 10^{12} \text{ s}^{-1}) \exp(-\Delta G^\ddagger/k_b T) \quad (17)$$

In light of the observation that for benzhydryl chloride the rate constant associated with the collapse of the CIP, k_1 , can be resolved kinetically, the temperature dependence of k_1 provides the associated activation parameters: for benzhydryl chloride in acetonitrile, $\ln(A) = 27.55 \pm 0.53 \text{ s}^{-1}$ ($A = 9.2 \times 10^{11} \text{ s}^{-1}$) and $E_a = 3.2 \pm 0.32 \text{ kcal/mol}$.⁹⁵ Defining κ as the ratio of the experimental pre-exponential factor, A_{exp} , to the transition-state theory pre-exponential factor, A_{TST} , yields

$$\kappa = (9.2 \times 10^{11} \text{ s}^{-1}) / (5.7 \times 10^{12} \text{ s}^{-1}) = 0.16 \quad (18)$$

Taking the experimental error for the A factor into account, the range in κ varies between 0.09 and 0.28. This value for κ places the system into the regime of polarization caging for the passage through the transition state; that is, the solvent's relaxation controls the dynamics of the passage. If this indeed true, then the passage through the transition state should depend upon the time scale associated with solvent relaxation, as reflected in the longitudinal relaxation time τ_1 . As the value of τ_1 for acetonitrile is 0.2 ps while the corresponding value for propionitrile is 0.3 ps, then the passage through the transition state in propionitrile should

Table 2. Activation Parameters, A and E_a , and the Value for κ Associated with Covalent Bond Formation, k_1 for Benzhydryl Chloride (BC), Benzhydryl Bromide (BB), 3,4'-Dimethoxybenzhydryl Acetate (MethoxyD+), 3-Methoxy-4'-methylbenzhydryl Acetate (MethylD+), and 3-Methoxybenzhydryl Acetate in Acetonitrile^a

compound	A^b ($\times 10^{12}$ s ⁻¹)	E_a^c (kcal/mol)	κ
BC	0.92	3.2	0.16
BB	0.49	3.0	0.15
MethoxyD+	5.5	5.4	1.0
MethylD+	0.51	3.2	0.09
D+	0.075	1.9	0.013

^a Values from ref 101. ^b Estimated error $\pm 50\%$. ^c Estimated error $\pm 20\%$.

be reduced by a factor of 1.5 relative to the case in acetonitrile. Indeed, comparing the experimentally derived A factors for benzhydryl chloride in acetonitrile and propionitrile, the A factor for propionitrile is reduced by a factor of 1.8, lending further support to the proposal that polarization caging by the solvent is controlling the passage through the transition state.⁹⁵

Table 2 presents the value of κ for the series of substituted benzhydryl derivatives thus far examined as well as the corresponding energies of activation for the collapse of the contact ion pairs. As the energies of activation decrease from 5.4 to 1.9 kcal/mol, the κ values also decrease from 1.0 to 0.013.¹⁰¹ To account for this behavior, it is proposed that as E_a decreases, there is a corresponding decrease in the reaction barrier frequency, ω_b , while for these systems the variation in the solvent frequency, ω_s , is assumed to be minimal. It is informative to compare the theoretical results for *tert*-butyl chloride in acetonitrile, where the reaction dynamics fall within the nonequilibrium solvation regime, with the benzhydryl systems where the reaction dynamics fall within the regime of polarization caging. While the reaction barriers for the collapse of the CIP are small in the benzhydryl systems, the theoretically derived barrier for the collapse of the CIP for *tert*-butyl chloride is rather large by comparison, 18 kcal/mol.¹³ This large barrier presumably leads to a large reaction barrier frequency, ω_b , relative to the solvent frequency, ω_s , so that $\omega_b \gg \omega_s$.

6.3. Solvent Control of Contact Ion Pair Separation

Our understanding of the parameters that control the process of contact ion pair diffusional separation to the solvent-separated ion pair in the S_N1 process has been based upon a limited number of experimental and the theoretical studies.¹⁰⁵ The first experimental report for the rate constants associated with the interconversion of a CIP with a SSIP that directly relates to the S_N1 mechanism is our study of the picosecond dynamics of the benzhydryl chloride ion pairs in acetonitrile.¹⁴ From the rate constant for CIP separation to SSIP ($k_2 = 2.9 \times 10^9$ s⁻¹) (Scheme 1) and the rate constant for the collapse of the SSIP to form the CIP ($k_3 = 1.3 \times 10^8$ s⁻¹), the free energy for the conversion of the CIP to the SSIP is found to be -1.8 kcal/mol in acetonitrile at room temperature; that is, the SSIP is more stable than the CIP in acetonitrile for this system.

However, prior to this study, there had been substantial progress in our understanding of how the solvent controls the relative energies of ionic species, contact relative to solvent-separated, and how the solvent controls the dynamics of their interconversions.^{106,107} These results were obtained

from numerous studies of photoinduced electron transfer between a donor and acceptor giving rise to contact and solvent-separated radical ion pairs.^{108–114}

The most insightful study into the solvent's influence on the relative energies of a contact radical ion pair (CRIP) and a solvent-separated radical ion pair (SSRIP) comes from Farid, Goodman, and Gould, who examined the radical ion pair interconversion of 1,2,4,5-tetracyanobenzene radical anion and the *p*-xylene radical cation.¹¹⁵ Weller has proposed that the free energies associated with the formation of the two radical ion pairs from the neutral species, ΔG_{RIP} , can be estimated on the basis of the oxidation potential of the donor, E_{D}^{ox} , and the reduction potential of the acceptor, $E_{\text{A}}^{\text{red}}$.^{116,117}

$$\Delta G_{\text{RIP}} = (E_{\text{D}}^{\text{ox}} - E_{\text{A}}^{\text{red}}) + \Delta_{\text{RIP}} \quad (19)$$

Δ_{RIP} for the CRIP is based upon the Onsager dipole model for the solvation of a dipole μ with a spherical radius r in a solvent characterized by its dielectric constant, ϵ .

$$\Delta_{\text{CRIP}} = \text{const} - (\mu^2/\rho^3)(\epsilon - 1)/(2\epsilon + 1) \quad (20)$$

Δ_{RIP} for the SSRIP is estimated from the Born model, where the average radius of the ions with a charge e_0 is r , their separation distance in the SSRIP is R_{DA} , and ϵ' is the dielectric constant of the solvent in which E_{D}^{ox} and $E_{\text{A}}^{\text{red}}$ were determined.

$$\Delta_{\text{SSRIP}} = (e_0^2/\epsilon)(r^{-1} - R_{\text{DA}}^{-1}) - (e_0^2/\epsilon')(r^{-1}) \quad (21)$$

From the measurement of the rate constants for the radical ion pair interconversion as a function of ϵ , Farid and co-workers found that the above models for the energies of the two forms of the radical ion pairs gave a good account of the relative free energies.¹¹⁵ Importantly, they observed that, for solvents with dielectric constants less than $\epsilon = 13$, the contact radical ion pair is more stable than the solvent-separated radical ion pair. The dielectric constants for the solvents examined ranges from $\epsilon = 7.2$ to $\epsilon = 24.6$. For $\epsilon = 7.2$, the SSRIP is less stable than the CRIP, i.e., $\Delta G(\text{CRIP} \rightarrow \text{SSRIP}) = 1.3$ kcal/mol. At the other extreme, $\epsilon = 24.6$, the SSRIP is more stable than the CRIP, i.e., $\Delta G(\text{CRIP} \rightarrow \text{SSRIP}) = -0.8$ kcal/mol.

The only in depth studies to date focusing upon the influence of solvent upon the dynamics of the passage through the transition for the separation of a contact ion pair are our experiments examining the diffusional separation of the *trans*-stilbene/fumaronitrile contact radical ion pair in a series of alkyl nitrile solvents.¹⁰⁷ On the basis of the temperature dependence of the rate constants for these processes, the associated activation parameters were analyzed within the context of Kramers theory. In the modeling, the Smoluchowski limit of the Kramers model was employed, where the solvent friction, ζ , is assumed to be proportional to the solvent viscosity, η . The model gave an excellent account of the observed temperature dependence of the rate constants. The derived intrinsic reaction barriers for contact ion pair separation are 0.80 kcal/mol for acetonitrile, 1.07 kcal/mol for propionitrile, 1.37 kcal/mol for butyronitrile, and 1.64 kcal/mol for pentanenitrile. The frequency associated with the passage through the transition state correlates with the inverse of the solvent viscosity, $1/\eta$, as expected for the hydrodynamic model for friction. These experimental

findings are consistent with the molecular dynamic simulations for ion pair separation undertaken by Hynes and co-workers, where they found that both the Kramer model and the Grote–Hynes model gave a good account of the transmission coefficient.⁹⁰

6.4. Parameters Controlling Nucleophilicity

Given that the rate constants for the collapse of the contact ion pair to produce a covalent bond as well as those associated with ion pair interconversion can be resolved for a variety of benzhydryl derivations, reaction diagrams for these processes are formulated in Figures 5 and 6. The

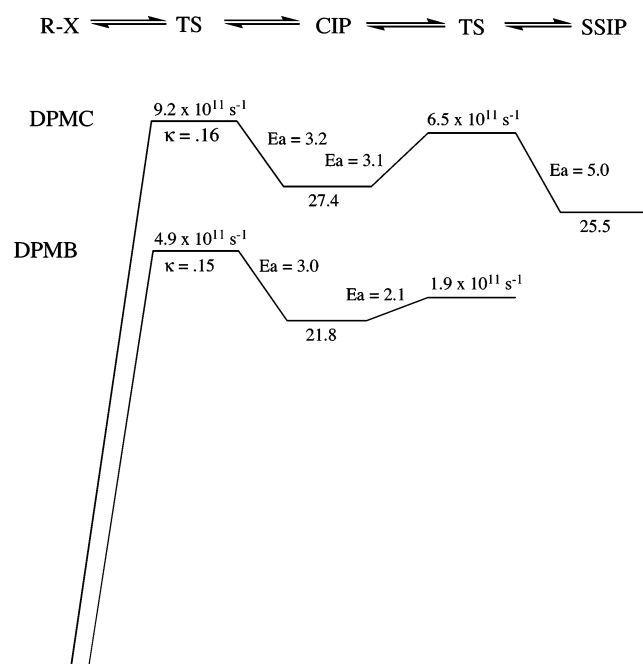


Figure 5. Reaction profile for benzhydryl chloride (DPMC) and benzhydryl bromide (DPMB) in acetonitrile. Energy in kcal/mole. Reprinted with permission from ref 101. Copyright 2005 American Chemical Society.

energies of the CIP relative to the initial reactant are obtained from electrochemical and thermochemical experiments as well as from electronic structure calculations.¹⁰¹ The activation parameters, E_a and A , as well as the κ factors are also displayed. With the development of these reaction profiles, we turn to the concept of nucleophilicity.

The concept of nucleophilicity is fundamental to the S_N1 reaction mechanism. As such, Ritchie developed the N^+ scale, based upon the relative reactivities of various nucleophiles with a given resonance stabilized cation, as a means to quantify nucleophilicity.²⁴ In recent years, the N^+ scale has been further expanded by Richard to include acetate (0.60), chloride (1.2), and bromide (2.2), with bromide being the better nucleophile.³⁴ It is important to emphasize that, within the context of the Winstein model for the S_N1 reaction mechanism, the nature of the Ritchie and Richard experiments reflects the sum of the individual kinetic processes as one molecular event. This would perhaps be valid if one of the many transformations in the mechanism was strongly rate determining.

With the resolution of the individual molecular events associated with the reaction of the various benzhydryl derivatives, one can begin to discuss the parameters that control reactivity. For example, on the basis of the N^+ scale

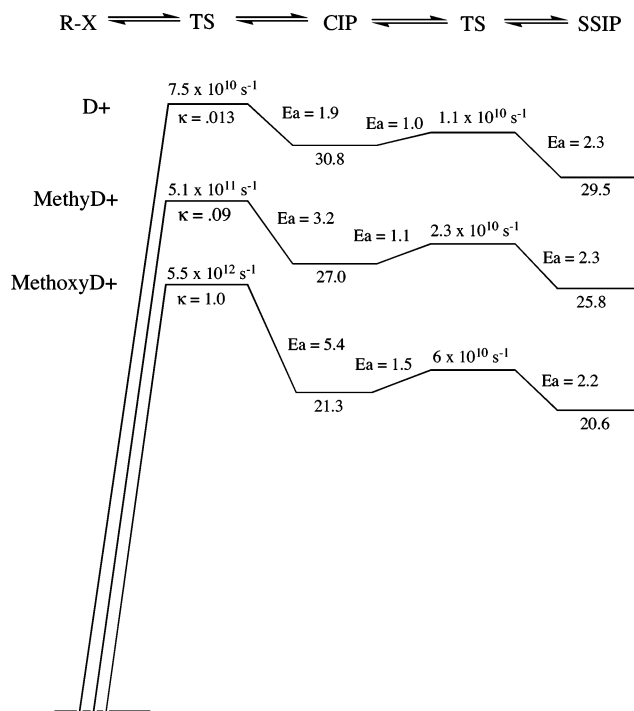


Figure 6. Reaction profile for 3-methoxybenzhydryl acetate (D+), 3-methoxy-4'-methylbenzhydryl acetate (MethylD+), and 3,4'-dimethoxybenzhydryl acetate (MethoxyD+) in acetonitrile. Energy in kcal/mole. Reprinted with permission from ref 101. Copyright 2005 American Chemical Society.

for bromide and chloride, bromide is the better of the two nucleophiles. Yet, the reaction of benzhydryl cation to form the covalent bond, k_1 , is faster with chloride, $3.8 \times 10^9 \text{ s}^{-1}$, than with bromide, $3.2 \times 10^9 \text{ s}^{-1}$ (Table 1). The origin of the enhanced reactivity of bromide relative to chloride, as reflected in N^+ , must then reside in the dynamics of ion pair interconversion. However, given the inability to resolve the kinetics associated with the collapse of the SSIP to form the CIP for the benzhydryl bromide, this issue is not addressed (Figure 5).

Another example illustrating the complexity of the problem of ascertaining the parameters that ultimately control nucleophilicity is found in the comparison of the rate constants associated with the collapse of the CIP giving rise to covalent bond formation in benzhydryl chloride and 3-methoxy-4'-methylbenzhydryl acetate. The overall energetics for the collapse of the CIP in these two molecular systems are virtually identical, 27 kcal/mol, and yet the rate constant for the chloride, $3.8 \times 10^9 \text{ s}^{-1}$, is also most a factor of 2 larger than the rate constant for the acetate, $2.2 \times 10^9 \text{ s}^{-1}$. The enhancement in the rate constant lies in the A factor not in the energies of activation, E_a , which are virtually identical for the two molecular systems (Table 2 and Figures 5 and 6). However, when the collapse of the CIP for benzhydryl bromide is compared with the case of 3,4'-dimethoxybenzhydryl acetate, again, processes occurring with the same overall energetics, the enhanced rate of the bromide is traced to a lower energy of activation and not an enhanced A factor (Table 2). Clearly, on the basis of these limited examples, understanding the parameters that control the relative ordering of nucleophilicity is less than straightforward. The study of many more molecular systems will be required to gain an understanding of the molecular parameters that control nucleophilicity.

7. Application of Marcus Theory to the S_N1 Mechanism

As a unifying framework for understanding the fundamental processes associated with the S_N1 reaction mechanism, Albery has proposed the implementation of Marcus theory as a means of analysis.³⁷ Marcus theory, originally developed for nonadiabatic electron-transfer processes, has found wide-ranging application in the study of organic reaction mechanisms.^{118–120} The most general form of Marcus theory establishes a quadratic relationship between the driving force for the reaction, ΔG , and the rate constant, k , for the process of interest.

$$k = A \exp\left(-\frac{\Delta G^\ddagger}{k_b T}\right) \quad \text{where} \quad \Delta G^\ddagger = \frac{(\Delta G + \lambda)^2}{4\lambda} \quad (22)$$

The parameter λ is the reorganization energy and is related to the free energy of activation at zero driving through the relationship $\Delta G^\ddagger = \lambda/4$. The identity of the A factor depends upon the nature of the molecular event under consideration. For nonadiabatic electron and proton transfer, the A factor is proportional to the matrix element associated with the tunneling process. For covalent bond formation, the A factor is related to the frequency associated with the passage through the transition state.

Following the suggestion that the Marcus formalism is fundamental to the S_N1 mechanism, Ritchie expressed reservations about its applicability.²⁵ In the original formulation of Marcus theory for electron transfer, the reorganization energy is obtained as the average of the reorganization energies for the two identity reactions. However, as Ritchie has pointed out, for nucleophilic addition reactions, no such relationship can be established. To circumvent this issue, it is feasible to identify the intrinsic barrier as $\lambda/4$ at $\Delta G = 0$. However, since most reactions studied do not occur at zero driving force, it is necessary to extrapolate to zero driving force by assuming a quadratic relationship between ΔG^\ddagger and ΔG as in eq 16 in order to deduce the rate constant at zero driving force; in the extrapolation procedure, it is assumed that the A factor is constant throughout the series of rate measurements. Ritchie questioned the validity of the quadratic relationship for nucleophilic addition for this relationship, as it is predicated upon parabolic potential energy surfaces for the reactant and product states. Theory suggests that an anharmonic potential would be more appropriate for bond heterolysis; an anharmonic potential will not yield a quadratic dependence. Indeed, in Hynes' theoretical study of *tert*-butyl chloride bond heterolysis in a polar solvent, they directly addressed this issue of the applicability of the quadratic dependence and found that it leads to an error of more than a factor of 2 in the determination of the reorganization energy.¹¹ Regarding the constancy of the A factor, we have shown that for a homologous series of reactions the A factor is not constant and can vary by as much as a factor of 73 (Figure 6).¹⁰¹

Finally, the S_N1 reaction mechanism for the benzhydryl derivatives is not kinetically dominated by one molecular event, but rather, numerous molecular processes significantly contribute to the overall rate of reaction (Figures 5 and 6). Thus, correlating the observed rate of the reaction with driving force to obtain a reorganization energy probably provides little insight into the nature of the parameters that govern the overall reactivity.

8. Concluding Remarks

When linear solvation energy relationships (LSER) for the solvent's influence upon the rate constant for solvolysis were developed, it was hoped that the analysis would provide insight into which properties of the solvent are critical in governing the dynamics of reaction. The formulation of LSER within the theoretical framework of transition-state theory normally involves relating $\log(k_1/k_2)$ to a function based on the molecular parameters (mp) characterizing the solvent, $f[\text{mp}]$, where $f[\text{mp}]$ is proportional to the difference in the free energy of activation for the two processes, $\Delta G_2^\ddagger - \Delta G_1^\ddagger$. To arrive at this relationship, the ratio of pre-exponential factors for the two rate processes is assumed to cancel, for in transition-state theory the influence of solvent is found only in the $\Delta G_2^\ddagger - \Delta G_1^\ddagger$ term. However, with the recent advances in our understanding of the influence that a solvent will have upon the passage through the transition state, as reflected in the pre-exponential factor, the act of cancellation of prefactors must be done with great caution. For example, in the benzhydryl molecular system, which has been extensively employed in solvolysis studies, the pre-exponential factors for bond heterolysis can vary by a factor of 73, over a range of $5.5 \times 10^{12} \text{ s}^{-1}$ to $7.5 \times 10^{10} \text{ s}^{-1}$. Furthermore, we now understand that the critical parameters governing the dynamics of reaction include not only ΔG^\ddagger but also the reaction barrier frequency, ω_b , the solvent frequency at the transition state, ω_s , and the solvent relaxation time, τ . At least for the benzhydryl molecular system, the application of the standard forms of LSER for the analysis of solvent effects upon reaction dynamics is called into question.

In assessing the events that control the reactivity of nucleophile–electrophile combination reactions, it has not been clear as to which of the molecular processes ultimately controls the reactivity. However, with the ability to time resolve the evolution of contact ion pairs and solvent-separated ion pairs for the benzhydryl derivatives, it is clear that no single molecular event is dominant but instead all of the processes associated with these ion pair species significantly contribute toward the overall reactivity. Given the difference in the nature of the molecular processes associated with covalent bond formation and ion pair interconversion, no single theory can capture the essence of nucleophilicity as was hoped for with the development of the N+ scale. Although the N+ scale has been a useful parameter for the correlation of extensive amounts of data, it in itself provides little insight into the molecular events that ultimately control nucleophilicity.

In a similar vein, the application of Marcus theory as a unifying formulation for nucleophilicity associated with reactions proceeding by the S_N1 mechanism is without foundation. Electronic structure theory has revealed that the form of the potential energy surfaces associated with covalent bond formation is not parabolic, a condition integral to Marcus theory. Furthermore, attempts to derive rate constants at zero driving force, required to obtain the reorganization energies, have also involved the assumption of a constant A factor provided by transition-state theory. With recent developments in the theory of solvent effects on the dynamics of transition state passage that have been supported by experiment, the assumption of a constant A factor is highly problematic.

Given that LSER have only provided confusing results in ascertaining the role of solvent in bond heterolysis in tertiary

systems, the question becomes, how is insight to be gained regarding the role of the solvent? The most promising avenue of investigation that will give us the most insight into the multidimensionality of the reaction path associated with bond heterolysis for tertiary systems resides in electronic structure calculations, explicitly taking into account the molecular nature of the solvent at the quantum level, coupled with molecular dynamic simulations. The level of sophistication that will be required for the calculations to provide reliable insights remains to be achieved.

9. Acknowledgments

Our studies are currently being supported by a grant of the National Science Foundation (No. CHE-0408265). I would also like to thank the undergraduates, graduate students, and postdoctoral fellows who have been involved in these studies for the past 10 years: Bulang Li, Ashok Deniz, Matthew Lipson, Jens Dreyer, Sarah Gasparrini, and Libby Heeb.

10. References

- Bateman, L. C.; Church, M. G.; Huges, E. D.; Ingold, C. K.; Taher, N. A. *J. Chem. Soc.* **1940**, 979.
- Bateman, L. C.; Hughes, E. D.; Ingold, C. K. *J. Chem. Soc.* **1940**, 1017.
- Bartlett, P. D.; Knox, L. H. *J. Am. Chem. Soc.* **1939**, *61*, 3184.
- Grunwald, E.; Winstein, S. *J. Am. Chem. Soc.* **1948**, *70*, 846.
- Winstein, S.; Clippinger, E.; Fainberg, A. H.; Robinson, G. C. *J. Am. Chem. Soc.* **1954**, *76*, 2597.
- Winstein, S.; Robinson, G. C. *J. Am. Chem. Soc.* **1958**, *80*, 169.
- Doering, W. v. E.; Zeiss, H. H. *J. Am. Chem. Soc.* **1953**, *75*, 4733.
- Neitzescu, C. D. Historical Outlook. In *Carbonium Ions*; Olah, G. A., Schleyer, P. v. R., Eds.; John Wiley & Sons: New York, 1968; Vol. 1; pp 1.
- Raber, D. J.; Harris, J. M.; Schleyer, P. v. R. Ions and Ion Pairs in Solvolysis Reactions. In *Ions and Ion Pairs in Organic Chemistry*; Szwarc, M., Ed.; John Wiley & Sons: New York, 1974; pp 248.
- Richard, J. P.; Amyes, T. L.; Toteva, M. M.; Tsuji, Y. Dynamics for the Reactions of Ion Pair Intermediates of Solvolysis. In *Advances in Physical Organic Chemistry*; Richards, J. P., Ed.; Elsevier: Amsterdam, 2004; Vol. 39, pp 1.
- Kim, H. J.; Hynes, J. T. *J. Am. Chem. Soc.* **1992**, *114*, 10508.
- Keirstead, W. P.; Wilson, K. R.; Hynes, J. T. *J. Chem. Phys.* **1991**, *95*, 5256.
- Kim, H. J.; Hynes, J. T. *J. Am. Chem. Soc.* **1992**, *114*, 10528.
- Peters, K. S.; Li, B. *J. Phys. Chem.* **1994**, *98*, 401.
- Ingold, C. K. *Proc. Chem. Soc.* **1957**, 279.
- Schadt, F. L.; Bentley, T. W.; Schleyer, P. v. R. *J. Am. Chem. Soc.* **1976**, *98*, 7667.
- Bentley, T. W.; Schleyer, P. v. R. *J. Am. Chem. Soc.* **1976**, *98*, 7658.
- Bentley, T. W.; Carter, G. E. *J. Am. Chem. Soc.* **1982**, *104*, 5741.
- Abraham, M. H.; Taft, R. W.; Kamlet, M. J. *J. Org. Chem.* **1981**, *46*, 3053.
- Farcasiu, D.; Jahme, J.; Ruchardt, C. *J. Am. Chem. Soc.* **1985**, *107*, 5717.
- Gajewski, J. J. *J. Am. Chem. Soc.* **2001**, *123*, 10877.
- Richard, J. P.; Toteva, M. M.; Amyes, T. L. *Org. Lett.* **2001**, *3*, 2225.
- Martinez, A. G.; Vilar, E. T.; Barcina, J. O.; Cerero, S. M. *J. Org. Chem.* **2005**, *70*, 10238.
- Ritchie, C. D. *Acc. Chem. Res.* **1972**, *5*, 348.
- Ritchie, C. D.; Kubisty, C.; Ting, G. Y. *J. Am. Chem. Soc.* **1983**, *105*, 279.
- Ritchie, C. D. *Can. J. Chem.* **1986**, *64*, 2239.
- Mayr, H.; Patz, M. *Angew. Chem., Int. Ed.* **1994**, *33*, 938.
- Minegishi, S.; Loos, R.; Kobayashi, S.; Mayr, H. *J. Am. Chem. Soc.* **2005**, *127*, 2641.
- McClelland, R. A.; Kanagasabapathy, V. M.; Steenken, S. *J. Am. Chem. Soc.* **1988**, *110*, 6913.
- Richard, J. P.; Amyes, T. L.; Toteva, M. M. *Acc. Chem. Res.* **2001**, *34*, 981.
- Richard, J. P.; Tsuji, Y. *J. Am. Chem. Soc.* **2000**, *122*, 3963.
- Toteva, M. M.; Richard, J. P. *J. Am. Chem. Soc.* **1996**, *118*, 11434.
- Richard, J. P.; Jencks, W. P. *J. Am. Chem. Soc.* **1984**, *106*, 1373.
- Richard, J. P.; Toteva, M. M.; Crugeiras, J. *J. Am. Chem. Soc.* **2000**, *122*, 1664.
- Tsuji, Y.; Toteva, M. M.; Garth, H. A.; Richard, J. P. *J. Am. Chem. Soc.* **2003**, *125*, 15455.
- Richard, J. P.; Williams, K. B.; Amyes, T. L. *J. Am. Chem. Soc.* **1999**, *121*, 8403.
- Albery, W. J. *Annu. Rev. Phys. Chem.* **1980**, *31*, 227.
- Ogg, R. A.; Polanyi, M. *Trans. Faraday Soc.* **1935**, *31*, 604.
- Baughan, E. C.; Evans, M. G.; Polanyi, M. *Trans. Faraday Soc.* **1941**, *37*, 377.
- Evans, A. G. *Trans. Faraday Soc.* **1946**, *42*, 719.
- Pross, A.; Shaik, S. S. *Acc. Chem. Res.* **1983**, *16*, 363.
- Pross, A. *Acc. Chem. Res.* **1985**, *18*, 212.
- Shaik, S. S. *J. Org. Chem.* **1987**, *52*, 1563.
- Shaik, S. S. *Pure Appl. Chem.* **1991**, *63*, 195.
- Shaik, S.; Shurki, A. *Angew. Chem., Int. Ed.* **1999**, *38*, 586.
- Warshel, A.; Weiss, R. M. *J. Am. Chem. Soc.* **1980**, *102*, 6218.
- Warshel, A. *Acc. Chem. Res.* **1981**, *14*, 284.
- Mathis, J. R.; Hynes, J. T. *J. Phys. Chem.* **1994**, *98*, 5445.
- Mathis, J. R.; Hynes, J. T. *J. Phys. Chem.* **1994**, *98*, 5460.
- Mathis, J. R.; Kim, H. J.; Hynes, J. T. *J. Am. Chem. Soc.* **1993**, *115*, 8248.
- Jorgensen, W. L.; Buckner, J. K.; Huston, S. E.; Rossky, P. J. *J. Am. Chem. Soc.* **1987**, *109*, 1891.
- Abraham, M. H. *J. Chem. Soc., Perkin Trans.* **1973**, *2*, 1893.
- Ingold, C. K. *Structure and Mechanism in Organic Chemistry*, 2nd ed.; Cornell University Press: Ithaca, NY, 1969.
- Westacott, R. E.; Johnston, K. P.; Rossky, R. J. *J. Am. Chem. Soc.* **2001**, *123*, 1006.
- Westacott, R. E.; Johnston, K. P.; Rossky, P. J. *J. Phys. Chem. B* **2001**, *105*, 6611.
- Kajimoto, O. *Chem. Rev.* **1999**, *99*, 355.
- Tucker, S. C. *Chem. Rev.* **1999**, *99*, 391.
- Winter, N.; Benjamin, I. *J. Phys. Chem. B* **2005**, *109*, 16421.
- Hartsough, D. S.; Merz, K. M. *J. Phys. Chem.* **1995**, *99*, 384.
- Okuno, Y. *J. Phys. Chem. A* **1999**, *103*, 190.
- Yamabe, S.; Tsuchida, N. *J. Comput. Chem.* **2004**, *25*, 598.
- Ford, G. P.; Wang, B. *J. Am. Chem. Soc.* **1992**, *114*, 10563.
- Eyring, H. *J. Chem. Phys.* **1935**, *3*, 107.
- Evans, M. G.; Polanyi, M. *Trans. Faraday Soc.* **1935**, *31*, 875.
- Wigner, E. P. *Trans. Faraday Soc.* **1938**, *34*, 1938.
- Steinfeld, J. I.; Francisco, J. S.; Hase, W. L. *Chemical Kinetics and Dynamics*; Prentice Hall: Englewood Cliffs, NJ, 1989.
- Truhlar, D. G.; Garrett, B. C.; Klippenstein, S. J. *J. Phys. Chem.* **1996**, *100*, 12771.
- Kosower, E. M. *An Introduction to Physical Organic Chemistry*; John Wiley & Sons: New York, 1968.
- Abraham, M. H. *Prog. Phys. Org. Chem.* **1974**, *11*, 2.
- Parker, A. J. *Chem. Rev.* **1969**, *69*, 1.
- Kramers, H. A. *Physica (The Hague)* **1940**, *7*, 284.
- Grote, R. F.; Zwan, G. v. d.; Hynes, J. T. *J. Phys. Chem.* **1984**, *88*, 4676.
- Grote, R. F.; Hynes, J. T. *J. Chem. Phys.* **1980**, *73*, 2715.
- Courteny, S. H.; Fleming, G. R. *J. Chem. Phys.* **1985**, *83*, 215.
- Sivakumar, N.; Hoburg, E. A.; Waldeck, D. H. *J. Chem. Phys.* **1989**, *90*, 2305.
- Courteny, S. H.; Fleming, G. R. *Chem. Phys. Lett.* **1984**, *103*, 443.
- Lee, M.; Bain, J.; McCarthy, P. J.; Han, C. H.; Haseltine, J. N.; Smith, A. B.; Hochstrasser, R. M. *J. Chem. Phys.* **1986**, *85*, 4341.
- Lee, M.; Haseltine, J. N.; Smith, A. B.; Hochstrasser, R. M. *J. Am. Chem. Soc.* **1989**, *111*, 5044.
- Bowman, R. M.; Eissenthal, K. B. *J. Chem. Phys.* **1988**, *89*, 762.
- Waldeck, D. H. *Chem. Rev.* **1991**, *91*, 415.
- Sun, Y. P.; Saltiel, J. J. *J. Phys. Chem.* **1989**, *93*, 8310.
- Lipson, M.; Peters, K. S. *J. Phys. Chem. A* **1998**, *102*, 1691.
- Bagchi, B.; Oxtoby, D. W. *J. Chem. Phys.* **1983**, *78*, 2735.
- Zwan, G. v. d.; Hynes, J. T. *J. Chem. Phys.* **1982**, *76*, 2993.
- Zwan, G. v. d.; Hynes, J. T. *J. Chem. Phys.* **1983**, *78*, 4174.
- Zichi, D. A.; Hynes, J. T. *J. Chem. Phys.* **1988**, *88*, 2513.
- Lee, S.; Hynes, J. T. *J. Chem. Phys.* **1988**, *88*, 6853.
- Fukui, K. *Acc. Chem. Res.* **1981**, *14*, 363.
- Ciccotti, G.; Ferrario, M.; Hynes, J. T.; Kapral, R. *Chem. Phys.* **1989**, *129*, 241.
- Ciccotti, G.; Ferrario, M.; Hynes, J. T.; Kapral, R. *J. Chem. Phys.* **1990**, *93*, 7137.
- Das, A. K.; Tembe, B. L. *J. Mol. Liq.* **1998**, *77*, 131.
- Olah, G. A.; Pittman, C. U.; Symons, M. C. R. Electronic Spectra. In *Carbonium Ions*; Olah, G. A., Schleyer, P. v. R., Eds.; John Wiley & Sons: New York, 1968; Vol. 1.
- Bartl, J.; Steenken, S.; Mayr, H.; McClelland, R. A. *J. Am. Chem. Soc.* **1990**, *112*, 6918.
- Zimmerman, H. E.; Sandel, V. R. *J. Am. Chem. Soc.* **1963**, *85*, 913.
- Deniz, A. A.; Li, B.; Peters, K. S. *J. Phys. Chem.* **1995**, *99*, 12209.
- Lipson, M.; Deniz, A. A.; Peters, K. S. *J. Phys. Chem.* **1996**, *100*, 3580.

- (97) Lipson, M.; Deniz, A. A.; Peters, K. S. *J. Am. Chem. Soc.* **1996**, *118*, 2992.
- (98) Lipson, M.; Deniz, A. A.; Peters, K. S. *Chem. Phys. Lett.* **1998**, *288*, 781.
- (99) Dreyer, J.; Peters, K. S. *J. Phys. Chem.* **1996**, *100*, 15156.
- (100) Dreyer, J.; Lipson, M.; Peters, K. S. *J. Phys. Chem.* **1996**, *100*, 15162.
- (101) Peters, K. S.; Gasparrini, S.; Heeb, L. R. *J. Am. Chem. Soc.* **2005**, *127*, 13039.
- (102) DeCosta, D. P.; Pincock, J. A. *J. Am. Chem. Soc.* **1989**, *111*, 8948.
- (103) Hilborn, J. W.; MacKnight, E.; Pincock, J. A.; Wedge, P. J. *J. Am. Chem. Soc.* **1994**, *116*, 3337.
- (104) Pincock, J. A. *Acc. Chem. Res.* **1997**, *30*, 43.
- (105) Kessler, H.; Feigel, M. *Acc. Chem. Res.* **1982**, *15*, 2.
- (106) Arnold, B. R.; Noukakis, D.; Farid, S.; Goodman, J. L.; Gould, I. R. *J. Am. Chem. Soc.* **1995**, *117*, 4399.
- (107) Li, B.; Peters, K. S. *J. Phys. Chem.* **1993**, *97*, 7648.
- (108) Ojima, S.; Miyasaka, H.; Mataga, N. *J. Phys. Chem.* **1990**, *94*, 5834.
- (109) Masuhara, H.; Mataga, N. *Acc. Chem. Res.* **1981**, *14*, 312.
- (110) Gould, I. R.; Noukakis, D.; Gomez-Jahn, L.; Young, R. H.; Goodman, J. L.; Farid, S. *Chem. Phys.* **1993**, *176*, 439.
- (111) Gould, I. R.; Farid, S. *Acc. Chem. Res.* **1996**, *29*, 522.
- (112) Angel, S. A.; Peters, K. S. *J. Phys. Chem.* **1991**, *95*, 3606.
- (113) Peters, K. S.; Lee, J. J. *J. Phys. Chem.* **1992**, *96*, 8941.
- (114) Peters, K. S. Diffusional. In *Ultrafast Dynamics of Chemical Systems*; Simon, J. D., Ed.; Kluwer Academic: Dordrecht, 1994.
- (115) Arnold, B. R.; Farid, S.; Goodman, J. L.; Gould, I. R. *J. Am. Chem. Soc.* **1996**, *118*, 5482.
- (116) Weller, A. Z. *Z. Phys. Chem. (Wiesbaden)* **1982**, *133*, 93.
- (117) Beens, H.; Knibbe, H.; Weller, A. *J. Chem. Phys.* **1967**, *47*, 1183.
- (118) Hine, J. *J. Am. Chem. Soc.* **1971**, *93*, 3701.
- (119) Guthrie, J. P. *J. Am. Chem. Soc.* **1991**, *113*, 7249.
- (120) Kurz, J. L. *J. Org. Chem.* **1983**, *48*, 5117.

CR068021K